Engineering Structures 88 (2015) 125–137

Contents lists available at ScienceDirect

Engineering Structures

journal homepage: www.elsevier.com/locate/engstruct

Extending modal pushover-based scaling procedure for nonlinear response history analysis of multi-story unsymmetric-plan buildings

Juan C. Reyes [a,*], Andrea C. Riaño [a], Erol Kalkan [b], Carlos M. Arango [a]

[a] Department of Civil and Environmental Engineering, Universidad de los Andes, Bogotá, Colombia
[b] Earthquake Science Center, United States Geological Survey, Menlo Park, CA, USA

ARTICLE INFO

Article history:
Received 12 July 2014
Revised 13 November 2014
Accepted 22 January 2015

Keywords:
Modal pushover-based scaling
Response history analysis
Unsymmetric-plan buildings

ABSTRACT

The modal-pushover-based-scaling (MPS) procedure has been developed for appositely selecting and scaling earthquake records for nonlinear response history analyses (RHAs) of multi-story symmetric-plan and single-story unsymmetric-plan buildings. This procedure is extended here to unsymmetric-plan buildings with significant torsional response under bi-directional earthquake excitations. The accuracy of the procedure is evaluated by using three-dimensional computer models of nine unsymmetric-plan buildings with 5, 10 and 15 stories. These models were subjected to nonlinear RHAs considering sets of seven far-field records selected and scaled according to the extended modal-pushover-based-scaling (EMPS) procedure. Structural responses were compared against benchmark values, defined as the median values of the engineering demand parameters (EDPs) due to a larger set of unscaled far-field records. Also examined here is the ASCE/SEI 7-10 scaling procedure for comparison purposes. This study clearly shows that the EMPS procedure provides much superior results in terms of accuracy (true estimates of expected median EDPs) and efficiency (reduced record-to-record variability of EDPs) than the ASCE/SEI 7-10 scaling procedure for far-field ground motions. Thus, the EMPS is deemed to be an appropriate procedure for nonlinear RHAs of multi-story unsymmetric-plan buildings.

1. Introduction

Performance-based procedures for evaluating existing buildings and proposed designs of new buildings in the U.S. require response history analyses (RHAs) for an ensemble of earthquake records in order to determine engineering demand parameters (EDPs) for validation of targeted performance criteria. Earthquake records selected for RHAs often need to be scaled to a seismic hazard level considered. Fraught with several challenging issues, selection and scaling of ground motions necessary for nonlinear RHA remains the subject of much research in recent years.

Among the many procedures proposed to modify ground motion records, the most widely used approaches are amplitude scaling and spectrum matching [1]. The objective of amplitude scaling procedures is to determine scaling factors for a small number of records such that the scaled records provide an accurate estimate of structural responses, and, at the same time are efficient, i.e. reduce the record-to-record variability (dispersion) of responses. The term "accuracy" means that the scaled records should provide median (or mean) responses close to the "exact" responses considering large population of records compatible with the hazard conditions specified. The term "efficiency" means that ground motions after scaling to the design (target) spectrum should impose similar seismic demands to the structure. While large record-to-record variability in EDPs leads to uncertainties in design and diminishes the confidence level, small record-to-record variability (dispersion) indicates that scaled records represents well the target demand level. Thus, a reliable scaling method should not only produce accurate but also efficient estimates of EDPs.

In earlier approaches, ground motion records were scaled to match a target intensity measure such as peak ground acceleration, effective peak acceleration, arias intensity, or effective peak velocity [2,3]. These approaches are generally inaccurate and inefficient for structures responding in the nonlinear range [3,4]. Scaling of records to match the target spectrum at the fundamental vibration period of the structure provides improved results for elastic structures whose response is dominated by its first-"mode" of vibration [5]. However, if the contributions of higher modes are important or the structure deforms significantly into the inelastic range, this scaling method becomes less accurate and less efficient [3,6,7]. Modifications of this method considering the target spectrum

* Corresponding author at: Department of Civil and Environmental Engineering, Universidad de los Andes, Cra 1 No. 18A-12, Bogotá, Colombia.
E-mail address: jureyes@uniandes.edu.co (J.C. Reyes).

http://dx.doi.org/10.1016/j.engstruct.2015.01.041
0141-0296/

ordinates at the first and second vibration periods have been proposed [8,9]; however, efficiency of these modified methods is compromised for near-fault records with a dominant velocity pulse [10]. To account for higher-mode contributions to response and lengthening of the apparent vibration period after the structure deforms into the inelastic range, the scaling factor for a ground motion record can be chosen to minimize the difference between its elastic response spectrum and the target spectrum over a period range [11–16]. Because the preceding methods do not consider explicitly the nonlinear behavior of the structure, they may not be appropriate for near-fault sites where the inelastic deformations can be significantly larger than the deformations of the corresponding linear system [7,17–19]. For such sites, scaling methods that are based on the inelastic deformation spectrum or consider the response of the first-"mode" inelastic single-degree-of-freedom (SDF) system are more appropriate [16,20,21]. These ideas were utilized by Kalkan and Chopra [22] to develop a modal-pushover-based-scaling (MPS) procedure for selecting and scaling earthquake ground motion records in a form convenient for evaluating existing structures and proposed designs of new structures. This procedure explicitly considers structural strength, determined from the first-"mode" pushover curve, and determines a scaling factor for each record to match a target value of the deformation of the first-"mode" inelastic SDF system. The MPS procedure has been proven to be accurate and efficient for low-, medium-, and high-rise buildings with symmetric plan [22–24] and ordinary standard bridges [25,26] subjected to one component of ground motion.

Scaling two horizontal components for use in three-dimensional (3D) analysis of buildings has received less attention. Researchers have proposed that both components of a record be scaled by the same factor, selected to match their geometric mean spectrum to the target spectrum over a period range [12,27]. For far-fault sites, the ASCE/SEI 7-10 standard [28] requires that the ground motion records be scaled so that the average value of the square-root-of-sum-of-squares (SRSS) spectra for all horizontal-component pairs does not fall below the target spectrum. Beyer and Bommer [27] present a comprehensive summary of various aspects that should be included in the process of selecting and scaling two components of ground motions. They conclude that selecting and scaling records according to their "goodness-of-fit" with the target spectrum leads to efficient estimates of median responses. Recently, Reyes and Chopra [29] extended the MPS procedure for one component of ground motion (mentioned above) to two horizontal components. In summary, most existing scaling procedures may not be appropriate for the following cases: (1) near-fault sites where the inelastic deformation can be significantly larger than the deformation of the corresponding linear system [3,4,7]; (2) tall buildings where the higher mode responses are significant [24]; (3) unsymmetric-plan buildings where various coupled lateral torsional vibration modes may provide comparable contributions to response. Clearly, there is a need to develop procedures for selection and scaling of ground motions to be used in nonlinear RHA of unsymmetric-plan buildings, ranging from low-rise to high-rise buildings subjected to multi-component ground motions.

Lastly, Reyes and Quintero [30] proposed a new version of the MPS procedure for single-story unsymmetric-plan buildings. In order to generalize the findings from single-story systems to multi-story systems, it is essential to perform further validation and verifications of the MPS procedure using realistic multi-degree-of-freedom (MDF) systems. This paper extends this procedure to multi-story unsymmetric-plan buildings. In addition, the developed procedure is compared against the ASCE/SEI 7-10 scaling procedure for far-field ground motions. Based on results from nine multi-story unsymmetric-plan buildings with various plan shapes and heights, it is shown that the EMPS procedure provides much superior results in terms of accuracy and efficiency than the ASCE/SEI 7-10 scaling procedure. This manuscript is the first study evaluating the ASCE7-10 and EMPS ground motion scaling procedure for irregular plan multi-story realistic structural systems. The ASCE7-10 procedure has been the common practice in U.S. for design verification of important structures, which often have irregular plans; thus, our study fills an important gap by showing the limitations of this ground motion scaling procedure and by examining its accuracy and efficiency considering various different types of plan irregular buildings.

2. Extended MPS procedure (EMPS)

3D analysis of buildings requires the use of the two horizontal components of the ground motion records. In current versions of the MPS procedure, the two components are scaled independently in order to increase the accuracy, efficiency and effectiveness of the method [29,30]. However, these investigations have been limited to the analysis of multi-story symmetric-plan and single-story un-symmetric plan buildings. In this investigation, the scale factors are estimated using roof displacements at the center of mass (C.M.) instead of deformation of the first-"mode" inelastic SDF system [30]. Scaling factor (*SF*) for each ground motion is obtained independently for each horizontal direction by solving the following nonlinear equation:

$$u_r - \hat{u}_r = 0 \tag{1}$$

where u_r is the peak roof displacement calculated by implementing the uncoupled modal response history analysis (UMRHA) [31, chapter 20], and $\hat{u}_r$ is the target roof displacement. In practical implementation, the target roof displacement may be estimated from the response spectrum by combining inelastic "modal" displacements, just as for linear systems. This application of modal combination rules to nonlinear systems obviously lacks a rigorous theoretical basis, but seems reasonable if the modes are weakly coupled [31, chapter 20].

The EMPS procedure is implemented here in three phases: (1) target roof displacement and pushover analyses, (2) scaling phase, and (3) selection phase. The step-by-step procedure is presented below in a general form, valid for 3D analysis of multi-story buildings.

2.1. Target roof displacement and pushover analyses

(1) For a given site, define the target spectra $\widehat{A}_x$ and $\widehat{A}_y$, in this study, taken as the median of the 5% damped pseudo-acceleration response spectra of two components of the records. For a selected earthquake scenario, it is commonly assumed that response spectra and EDPs are log-normally distributed [32]. For this reason, it is more appropriate to represent the "mean" structural response by the median; a conclusion that is widely accepted. Because the geometric mean and median of a random variable having a log-normal distribution are the same, we decided to employ the term "median" instead of geometric mean, as is commonly done.
The use of the median spectrum as the target spectrum is not a constraint of the proposed EMPS procedure; any other target spectrum (e.g., 84th percentile target spectrum) can be utilized.

(2) Compute the natural frequencies ω_n (periods T_n) and modes ϕ_n of the first few modes of linear-elastic vibration of the building. For each ground motion component direction (x or y), identify the first, second and third modes as the three modes with the largest effective modal mass.

(3) Develop the base shear-roof displacement, $V_{bn} - u_{rn}$, relation or pushover curve by nonlinear static analysis of the building subjected to the n^{th}-"mode" invariant force distribution [33–35]:

$$s_n^* = \begin{bmatrix} \mathbf{m}\phi_{xn} \\ \mathbf{m}\phi_{yn} \\ \mathbf{I}_o\phi_{\theta n} \end{bmatrix}$$

where $\mathbf{m}$ is a diagonal matrix of order N with $m_{jj} = m_j$, the mass lumped at the j^{th} floor level; $\mathbf{I}_o$ is a diagonal matrix of order N with $I_{ojj} = I_{oj}$, the moment of inertia of the j^{th} floor diaphragm about a vertical axis through the center of mass (C.M.); and subvectors ϕ_{xn}, ϕ_{yn}, and $\phi_{\theta n}$ of the n^{th} mode ϕ_n represent x, y and θ components of ground motion, respectively. Gravity loads are applied before the lateral forces causing lateral displacement u_{rg} at the roof. This step should be implemented only for the first three "modes" in the direction under consideration; this step may be omitted for the higher-"modes" if they are treated as linear-elastic [31, chapter 20].

(4) Idealize the $V_{bn} - u_{rn}$ pushover curve as a bilinear or trilinear curve, as appropriate, and convert it into the force–deformation, $(F_{sn}/L_n) - D_n$, relation for the n^{th}-"mode" inelastic SDF system using well-known relationships [31, chapter 20]:

$$\frac{F_{sn}}{L_n} = \frac{V_{bn}}{M_n^*} \quad D_n = \frac{u_{rn}}{\Gamma_n \phi_{rn}}$$

where F_{sn} is a nonlinear hysteretic function of the n^{th} modal coordinate, M_n^* the effective modal mass for the n^{th}-"mode",

$$\Gamma = \frac{L_n}{M_n} = \frac{\phi_n^T \mathbf{M} \iota}{\phi_n^T \mathbf{M} \phi_n} \quad \mathbf{M} = \begin{bmatrix} \boldsymbol{m} & 0 & 0 \\ 0 & \boldsymbol{m} & 0 \\ 0 & 0 & \boldsymbol{I}_o \end{bmatrix} \quad \iota_x = \begin{bmatrix} \mathbf{1} \\ \mathbf{0} \\ \mathbf{0} \end{bmatrix} \quad \iota_y = \begin{bmatrix} \mathbf{0} \\ \mathbf{1} \\ \mathbf{0} \end{bmatrix}.$$

$\mathbf{1}$ and $\mathbf{0}$ are vectors of dimension N with all elements equal to one and zero, respectively. ϕ_{rn} is the value of ϕ_n at the C.M. of the roof. Starting with this initial loading curve, define the unloading and reloading branches appropriate for the structural system and material being considered. Recall that this step should be implemented only for the first three "modes" in the direction under consideration.

(5) Establish the target value of roof displacement $\hat{u}_r$. For a system with known vibration period T_n, damping ratio ζ_n, and force–deformation curve (step 3), determine the peak deformation D_n for the n^{th}-"mode" inelastic SDF system due to each of the unscaled ground motions $\ddot{u}_g(t)$ by solving:

$$\ddot{D}_n(t) + 2\zeta_n\omega_n\dot{D}_n(t) + \frac{F_{sn}}{L_n} = -\ddot{u}_g(t) \rightarrow D_n$$

Multi-story buildings may be treated as linearly elastic in computing the peak deformation D_n for "modes" higher than the first three "modes". Compute $\widehat{D}_n$ as the median of the D_n values. Compute roof displacement in the direction under consideration of the n^{th}-"mode" as

$$\hat{u}_{rn} = \Gamma_n \phi_{rn} \widehat{D}_n$$

Compute the roof displacement in the direction under consideration $\hat{u}_r$ from values of $\hat{u}_m$ using a suitable modal combination method (e.g., complete quadratic combination). In practical applications, target deformation $\widehat{D}_n$ can be computed as $\widehat{D}_n = C_{Rn}\widehat{D}_{no}$, where C_{Rn} is the inelastic deformation ratio, estimated from empirical equations [19], $\widehat{D}_{no} = (T_n/2\pi)^2\widehat{A}_n$, and $\widehat{A}_n$ is the target pseudo-spectral acceleration at period T_n. However, in this study, the deformation $\widehat{D}_n$ was computed as the median value of the peak deformations of the first-"mode" inelastic SDF system due to an ensemble of unscaled records; our interest is to test the proposed EMPS procedure, not existing C_{Rn} equations [29].

2.2. Scaling phase

(6) Compute the scale factor SF for each record in the direction under consideration solving the following nonlinear equation:

$$u_r - \hat{u}_r = 0$$

where u_r is the peak roof displacement at the C.M. in the direction under consideration due to the scaled records. Because this equation is nonlinear, SF cannot be determined a priori, but requires an iterative procedure as shown below:

a. Select an initial value of the scale factor SF, and compute deformation $D_n(t)$ for the n^{th}-"mode" inelastic SDF due to the scaled record by solving:

$$\ddot{D}_n(t) + 2\xi_n\omega_n\dot{D}_n(t) + \frac{F_{sn}}{L_n} = -SF \times \ddot{u}_g(t) \rightarrow D_n(t)$$

b. Compute roof displacement of the n^{th}-"mode" in the direction under consideration:

$$u_{rn}(t) = \Gamma_n \phi_{rn} D_n(t)$$

c. Compute roof displacement in the direction under consideration:

$$u_r = max\left(\left|\sum_n u_{rn}(t)\right|\right)$$

d. Estimate error: $\varepsilon = u_r - \hat{u}_r$

e. Adjust the value of the scale factor SF, and repeat steps "a" to "d" until ε is less than a tolerance value.

In this study, step "e", which must be implemented for all records, was implemented by a numerical algorithm. By developing steps "a" to "e", separately for the x and y components of the record, scale factors SF_x and SF_y are determined. Note that pushover curves (step 3), and target roof displacement (step 5) will be different for the two horizontal components [34,35]. Reyes and Chopra [29] demonstrated that it may not be possible to achieve accurate estimates of EDPs if both horizontal components of a record are to be scaled by the same factor, unless the only records selected are those that the peak floor displacement due to each unscaled component is close to the target value. Unfortunately, such a restriction will reduce the number of useable records and, in particular, eliminate near-fault records because their fault-normal and fault-parallel components are known to be very different due to directivity effects and fling [36]. Furthermore, such a constraint may not achieve the desired objectives of accuracy and efficiency if the target roof displacements in the two directions are very different because of different lateral-force-resisting systems. To overcome these restrictions, two different scaling factors for the two components of a record is an alternative option. Seismologists may find this approach to be questionable because it does not preserve focal mechanism and wave travel path effects, inherent in recorded motions. However, if the goal of any scaling procedure is to estimate the EDPs accurately—where the benchmark values are determined from a large set of unscaled records, which obviously preserve all the seismological features then such an approach is justified [29].

2.3. Selection phase

(7) Select the first k records with the lower values of:

$$Error = \sum_{i=4}^{6}\left(\left|SF_x A_x(T_i) - \widehat{A}_x(T_i)\right| + \left|SF_y A_y(T_i) - \widehat{A}_y(T_i)\right|\right)$$

where $\widehat{A}_x$ and $\widehat{A}_y$ are vectors of spectral values $\widehat{A}_i$ at different periods T_i ($T_i = T_4, T_5, T_6$,); A_x and A_y are vectors of spectral values for the unscaled records over the same period values. The selection phase considers the higher modes to select the final set of records to be used in RHAs. The first k records with the lower values of the equation shown above will be those whose spectrum best fits the target spectrum in the periods T_4, T_5, and T_6. In this study, we use $k = 7$.

The procedure presented differs from the MPS procedure for single-story unsymmetric plan buildings [30] in the selection phase. In this study, selection was made considering spectrum shape only at periods T_4, T_5 and T_6, not in the range from $0.2T_1$ to $1.5T_1$. In building codes, nonlinear RHA is not for preliminary design, but verification of final design of special structures (such as tall or irregular buildings), structures with innovative structural systems and materials, or structures on soft soil. In such structures, common practice is to complete elastic code-based design first, and then conduct nonlinear static analysis for validation of performance objective. Nonlinear RHA is conducted at the final stage for validation and verification. Because nonlinear static analysis is conducted as "a priori", the strength and deformability of the structure becomes available for scaling records according to the EMPS procedure.

3. ASCE/SEI 7-10 scaling procedure for far-field ground motions

For far-field ground motions, the ASCE/SEI 7-10 standard (henceforth abbreviated as ASCE7) requires that both components of an earthquake record be scaled by the same factor, determined to ensure that the average of the SRSS response spectra over all records does not fall below the corresponding ordinate of the target spectrum over the period range $0.2T_1$ to $1.5T_1$. The SRSS spectrum is computed for the 5%-damped response spectra for the two horizontal components of ground motion. The design value of an EDP—member forces, member deformations, story drifts, etc.—is taken as the average value of the EDP if at least seven scaled records are used in the analyses, or the maximum value of the EDP, otherwise. Various combinations of scaling factors for individual records can satisfy the preceding requirement for the average SRSS response spectrum. To achieve the desirable goal of scaling each record by a factor as close to one as possible, the ASCE7 procedure was implemented using a modified version of the approach described in Appendix A of Ref. [29]. The records were selected by minimizing the discrepancy between the scaled spectrum of a record and the target spectrum over the period range from $0.2T_1$ to $1.5T_1$, and then identifying the final set of records as those with spectral acceleration values at T_1 close to the target spectrum. This selection procedure was proposed by Reyes and Kalkan [37,38] and is not part of the requirements of the ASCE7. In the implementation of the ASCE7 procedure, the target pseudo-acceleration spectrum was taken as the average of the target spectra for both horizontal components.

4. Ground motions selected

The 30 records selected for this investigation (listed in Table 1) were recorded from seven shallow crustal earthquakes with moment magnitude $M_W = 6.7 \pm 0.2$, at distances (R_{JB}) ranging from 20 to 30 km, and with NEHRP site classification C (very dense soil or soft rock) or D (stiff soil). Because the ground motions selected were not intense enough to drive the buildings considered far into the inelastic range—an obvious requirement to test any scaling procedure—they were pre-amplified by a factor of 4.0. These pre-amplified ground motions are treated as "unscaled" records for this investigation. Shown in Fig. 1 are the 5%-damped median response spectra for x and y components of the original ground motions. The median spectrum is taken as the target spectrum for purposes of evaluating the EMPS and other scaling procedures. It should be noted that our objective was to create a sample of records from a representative subset of a population of already recorded and not yet recorded ground motions under similar magnitude, distance and site conditions. The best way to avoid a biased or unrepresentative sample is to select a random sample. Therefore, selection of 30 records from the representative subset of the population was conducted randomly. This process statically allows us to treat the median spectrum of this random sample as the "true" target spectrum. Because all records were up-scaled with the same scaling factor, the assumption of random sampling was not violated.

The structures were subjected to sets of seven records scaled according to the EMPS and ASCE7 procedures, and their responses were compared against the benchmark values, defined as the median values of the EDPs obtained from nonlinear RHA of the structure subjected to 30 unscaled records [23,25,29,30,39–42]. These records are from multiple events, and their spectral shapes show significant aleatoric variability (Fig. 1). We believe that this large randomly populated set provides unbiased estimates of "true" (expected) median response considering the hazard conditions specified.

5. Structural systems

The structures considered are nine un-symmetric plan hypothetical buildings with 5, 10 and 15 stories. These buildings were designed according to the 2009 International Building Code [43] to be located in Los Angeles, California, and they cover the levels of horizontal irregularity defined in the ASCE7. The lateral resisting system of the buildings consists of steel special moment resisting frames (SMRF). Their plan shapes are shown in Fig. 2, where the moment resisting frames are highlighted. The buildings are identified by the letters R, L and T followed by the number of stories: plan R is approximately rectangular, plan T is symmetric about the y axis, and plan L is un-symmetric about both x and y. The buildings have similar plan areas and floor weights, with a span length of 30 ft (9.14 m) and a story height of 10 ft (3.05 m). The earthquake design forces were determined by bi-directional linear response spectrum analysis of the building with the design spectrum reduced by a response modification factor $R = 8$. However, member sizes were governed by drift limits instead of strength requirements.

To verify that the selected buildings cover a broad range of torsional irregularities, the following factor was calculated for each building [28]:

$$\beta = \Delta_{max}/\Delta_{average} \tag{2}$$

where Δ_{max} is the maximum story drift and $\Delta_{average}$ is the average story drift at the two ends of the structure. The level of torsional irregularity was qualified as recommended in the ASCE7 standard as:

(i) Not torsional irregularity: $\beta < 1.2$,
(ii) Torsional irregularity: $1.2 \leqslant \beta \leqslant 1.4$ and,
(iii) Extreme torsional irregularity: $\beta > 1.4$.

The buildings selected cover these three levels of torsional irregularity as demonstrated in Table 2, where the values of irregularity factor β are shown in ascending order. Fig. 3, showing

Table 1
List of 30 far-field ground motion records.

ID	Earthquake name	Year	Station name	M_w	R_{JB} (km)	NEHRP site class
1	San Fernando	1971	LA – Hollywood Stor FF	6.6	22.8	D
2	San Fernando	1971	Santa Felita Dam (Outlet)	6.6	24.7	C
3	Imperial Valley-06	1979	Calipatria Fire Station	6.5	23.2	D
4	Imperial Valley-06	1979	Delta	6.5	22.0	D
5	Imperial Valley-06	1979	El Centro Array #1	6.5	19.8	D
6	Imperial Valley-06	1979	El Centro Array #13	6.5	22.0	D
7	Imperial Valley-06	1979	Superstition Mtn Camera	6.5	24.6	C
8	Irpinia, Italy-01	1980	Brienza	6.9	22.5	C
9	Superstition Hills-02	1987	Wildlife Liquef. Array	6.5	23.9	D
10	Loma Prieta	1989	Agnews State Hospital	6.9	24.3	D
11	Loma Prieta	1989	Anderson Dam (Downstream)	6.9	19.9	C
12	Loma Prieta	1989	Anderson Dam (L Abut)	6.9	19.9	C
13	Loma Prieta	1989	Coyote Lake Dam (Downst)	6.9	20.4	D
14	Loma Prieta	1989	Coyote Lake Dam (SW Abut)	6.9	20.0	C
15	Loma Prieta	1989	Gilroy Array #7	6.9	22.4	D
16	Loma Prieta	1989	Hollister – SAGO Vault	6.9	29.5	C
17	Northridge-01	1994	Castaic – Old Ridge Route	6.7	20.1	C
18	Northridge-01	1994	Glendale – Las Palmas	6.7	21.6	C
19	Northridge-01	1994	LA – Baldwin Hills	6.7	23.5	D
20	Northridge-01	1994	LA – Centinela St	6.7	20.4	D
21	Northridge-01	1994	LA – Cypress Ave	6.7	29.0	C
22	Northridge-01	1994	LA – Fletcher Dr	6.7	25.7	C
23	Northridge-01	1994	LA – N Westmoreland	6.7	23.4	D
24	Northridge-01	1994	LA – Pico & Sentous	6.7	27.8	D
25	Kobe, Japan	1995	Abeno	6.9	24.9	D
26	Kobe, Japan	1995	Kakogawa	6.9	22.5	D
27	Kobe, Japan	1995	Morigawachi	6.9	24.8	D
28	Kobe, Japan	1995	OSAJ	6.9	21.4	D
29	Kobe, Japan	1995	Sakai	6.9	28.1	D
30	Kobe, Japan	1995	Yae	6.9	27.8	D

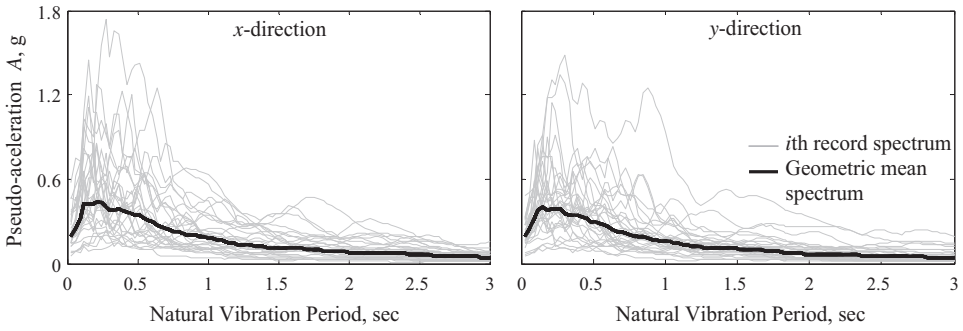

Fig. 1. Geometric-mean pseudo-acceleration response spectra of 30 records for 5% damping; individual response spectra of the records are also shown.

effective modal masses of the buildings permits the following observations: (1) Lateral displacements dominate motion of the R-plan and L10 buildings in modes 1 and 2, whereas torsion dominates motion in the third mode, indicating weak coupling between lateral and torsional components of motion. (2) Coupled lateral-torsional motions occur in the first and third mode of L05, T05 and T10 buildings whereas lateral displacements dominate motion in the second mode. (3) Lateral displacement dominates motion in the first mode, whereas coupled lateral-torsional motions occur in the second and third mode of T15 plan. For these reasons, it is expected that the contribution of higher modes be important in the selection and modification of seismic records, especially in structures where the effective mass of the fundamental mode is low. Note that all these conclusions are drawn from linear analysis; nonlinear behavior may attenuate or increase the lateral torsional motions of the buildings. Further details of the structural systems including their fundamental periods, mode shapes, etc. can be found in Refs. [40–42].

Nonlinear RHA and pushover analyses for these buildings were conducted using PERFORM-3D [44]. The following features were used in modeling the buildings: (1) girders and columns were modeled by a linear element with tri-linear plastic hinges at the ends of the elements that can include in-cycle strength deterioration, but not cyclic stiffness degradation; axial load-moment interaction for the columns was based on plasticity theory; (2) panel zones were modeled as four rigid links hinged at the corners with a rotational spring that represents the strength and stiffness of the connection; (3) ductility capacities of girders, columns, and panel zones were specified according to the ASCE/SEI 41-06 standard [45]; (4) columns of moment resisting frames were assumed to be fixed at the base, whereas gravity columns were considered pinned at the base; and (5) effects of nonlinear geometry were approximated by a standard P–Δ formulation for both moment and gravity frames.

6. Evaluating EMPS and ASCE7-10 procedures

The EMPS and ASCE7 procedures were implemented to select and scale sets of seven records; the evaluation procedure used in this paper was also used in Refs. [23,29,30,39–42]. In this paper,

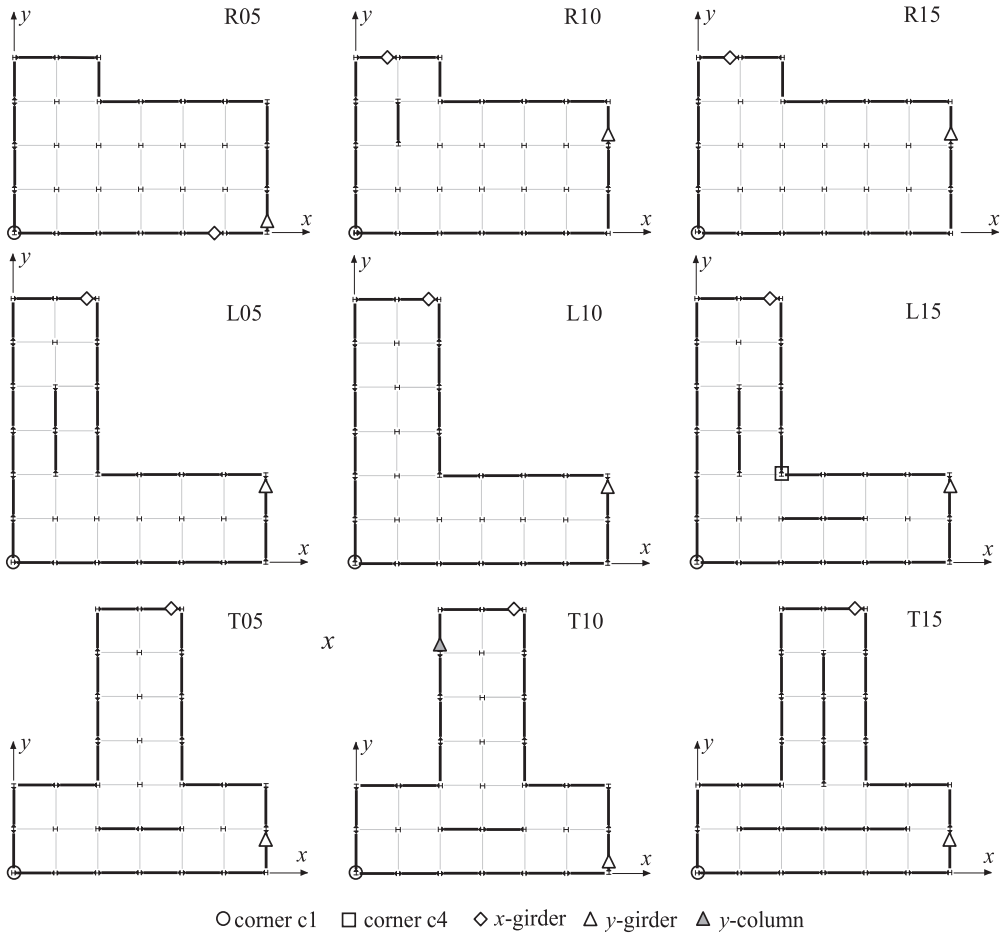

Fig. 2. Plan views of nine unsymmetric-plan buildings.

Table 2
Torsional irregularity factors.

Building	R05	R15	R10	L10	L15	T15	L05	T10	T05
β	1.00	1.10	1.13	1.20	1.26	1.30	1.35	1.41	1.43

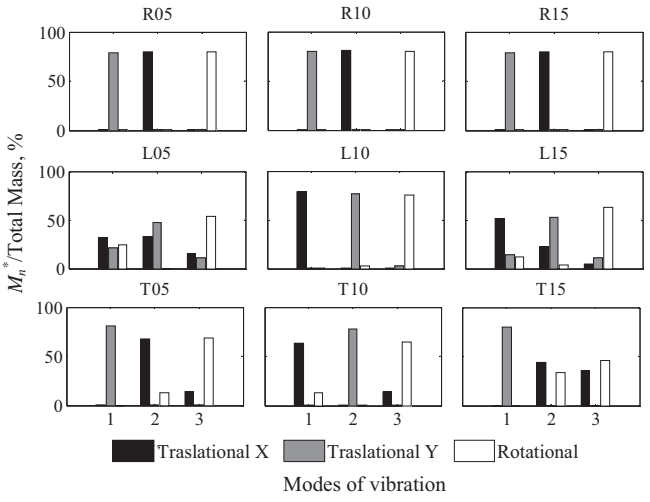

Fig. 3. Effective modal masses M_n^* of buildings selected.

it is assumed that the EDPs are log-normally distributed. This assumption was tested by constructing probability plots of various EDPs. As an example, Fig. 4 shows a probability plot of first story drift values obtained at the C.M. of the L15 building. It is evident that data are log-normally distributed because they follow a linear trend; therefore, it is appropriate to represent the "mean" response by the geometric mean (or median), instead of the average [46]. For a log-normal distribution of a random variable, the geometric mean ($\hat{\mu}$) and median (x_{50}) are given by the same equation: $x_{50} = \hat{\mu} = e^{\mu}$, where μ is the mean of a log-normal distribution. Therefore, it is not misleading to use median instead of geometric mean.

The MPS procedure proposed by Reyes and Chopra [29] (called here "MPS-Sym") was developed and tested only for multi-story symmetric-plan buildings. If this procedure is applied to the unsymmetric-plan buildings of this investigation, the results are not satisfactory as shown in Fig. 5 where story shears in *y*-column (Fig. 2), normalized by peak values occurring at any floor from set MPS-Sym are plotted against benchmark values (denoted as "Bench") for building T10; this figure also includes the results of the proposed procedure (set EMPS). It is evident that set EMPS lead to more accurate estimates of EDPs and lower record-to-record variability than set MPS-sym demonstrating that the proposed EMPS method is more appropriate for multi-story unsymmetric-plan buildings. These conclusions are also valid for the other buildings and EDPs considered in this research.

In the scaling phase of the EMPS procedure, the scale factor *SF* for each record in the direction under consideration is determined by solving Eq. (1). In order to evaluate the accuracy of the EMPS

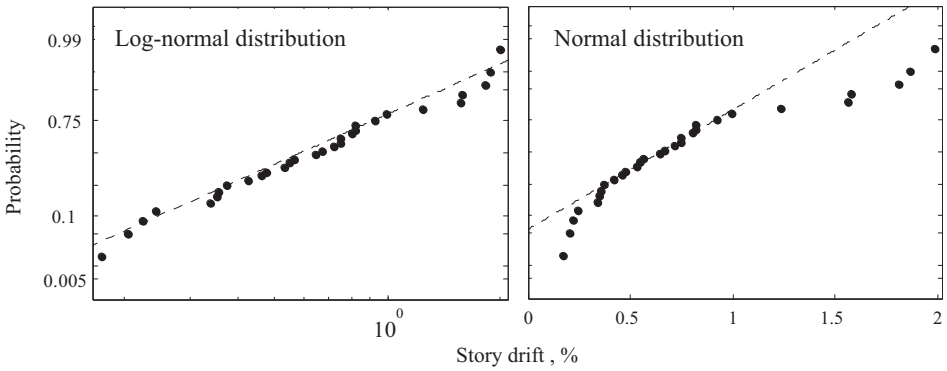

Fig. 4. Probability plot of first story drifts at the C.M. of structure L15 subjected to 30 ground motion records.

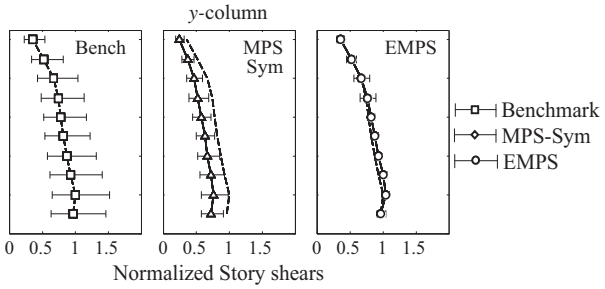

Fig. 5. Normalized story shears in *y*-column for T10 structure (see Fig. 2). In each case, the marker and the horizontal line represent the median value of the EDP ± one standard deviation σ assuming a log-normal distribution; benchmark EDP is repeated as dashed line for comparison.

procedure in the prediction of the roof displacement, Fig. 6 shows the resultant roof displacement time series calculated by step 6 of the EMPS procedure [30] and by nonlinear RHA of the building subjected to bi-directional ground motions for record #7 in Table 1; also included in the figure are target roof displacements obtained from step 5 of the EMPS procedure (horizontal dashed line $\hat{u}_r$) and from nonlinear RHA of the building subjected to 30 un-scaled ground motions (horizontal solid line $\hat{u}_{r\text{Perform3D}}$). The later corresponds to the exact value of the target roof displacement. It is evident that the EMPS procedure approximately resembles roof displacement time series, and adequately determines target and maximum roof displacements.

The EMPS procedure considers only modal responses in the direction of analysis. To demonstrate that the EMPS procedure is accurate in determining the maximum roof displacement, even in structures with modes having large modal participation factors in *x* and *y* directions, the following example was developed for building L15. We selected this building because the modal participation factors Γ_n in the *x*-direction are: 0.872, 0.574 and −0.345 for the first, second and third modes with largest modal effective mass (modes used in the EMPS procedure) and in *y*-direction are −0.459, 0.887 and 0.172. Fig. 7 shows the roof displacement time series in *x*-direction calculated by step 6 of the EMPS procedure and by nonlinear RHA of the building subjected to bi-directional excitation using two ground motion components of record #7. For the EMPS procedure, this figure includes *x*-direction displacement as a result of the *x*-component of the ground motion (u_{xx} in Fig. 7a), and also as a result of the *y*-component of the ground motion (u_{xy} in Fig. 7b); Fig. 7c presents the total response $u_{rx} = u_{xx} + u_{xy}$. The exact *x*-displacement calculated by PERFORM-3D is included in subplots (a) and (c) as a bold line. Comparing the EMPS results u_{xx} with the exact values $(u_x)_{\text{Perform3D}}$ obtained from PERFORM-3D, it is evident that even in structures with modes having large modal participation factors in both horizontal directions, the EMPS procedure leads to accurate estimates of the maximum roof displacement considering only the 3 modes with larger effective modal mass and the modal response in the direction of study (*x*-direction in this case). This is due to the fact that maximum values in the direction of analysis appear at different times when the structure is subjected to *x*- or *y*-component of ground motion. Similar results were observed for the other eight buildings analyzed; these results are not shown due to space limitations.

6.1. R-plan structures

For R-plan structures having 5, 10 and 15 stories, Figs. 8 and 9 show story drifts at corner c1 (see Fig. 2) and floor velocities at the C.M. The floor velocities are normalized by peak values occurred at any floor. First, second and third columns of these figures show EDP values in *x*-direction for the benchmark, ASCE7 and EMPS procedures, respectively; the next three columns show

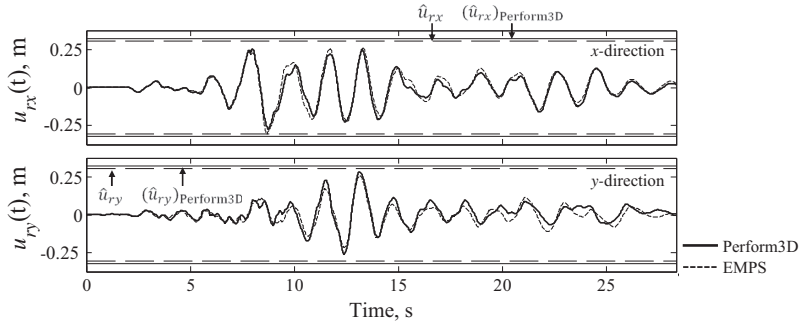

Fig. 6. Roof displacement time series in *x* and *y* directions at the C.M. for L15 building subjected to record #7: EMPS estimates vs. exact values.

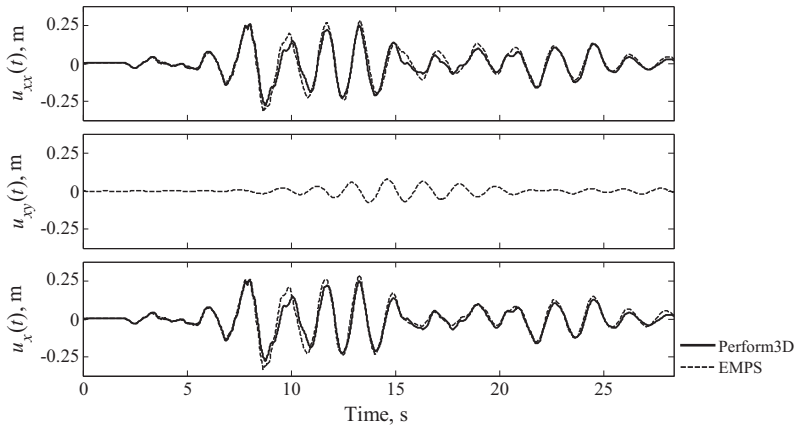

Fig. 7. Roof displacement time series in *x*-direction at the C.M. for L15 building.

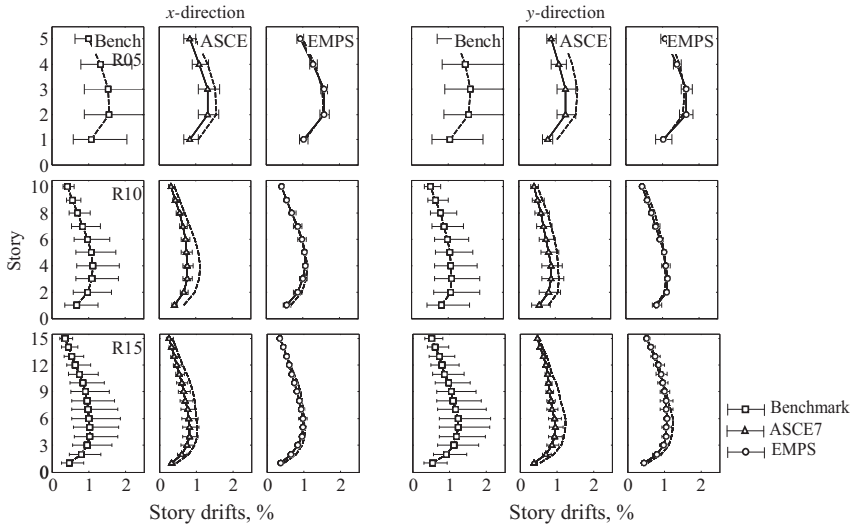

Fig. 8. Story drifts in percentage in *x*- and *y*-direction at corner c1 for R-plan structures. In each case the marker and the horizontal line represent the median value of the EDP ± σ, assuming a log-normal distribution.

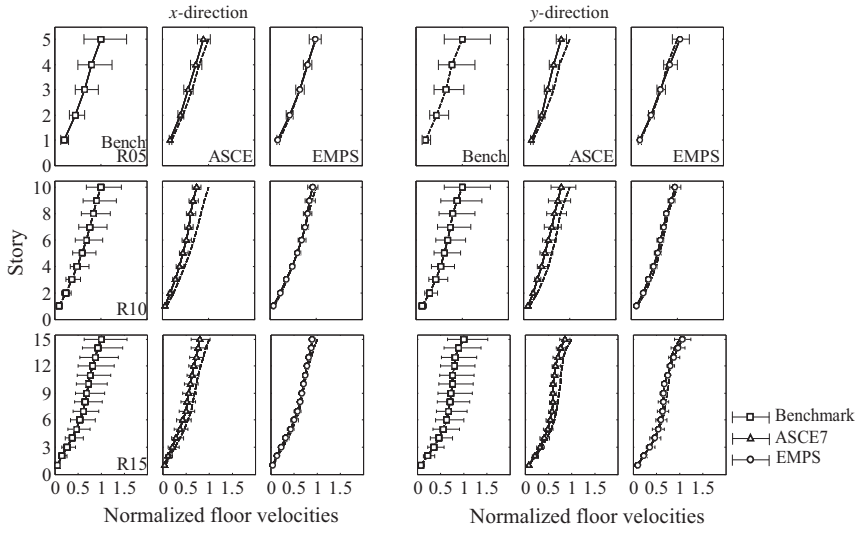

Fig. 9. Normalized floor velocities at the center of mass in *x*- and *y*-direction for R-plan structures. In each case the marker and the horizontal line represent the median value of the EDP ± σ, assuming a log-normal distribution.

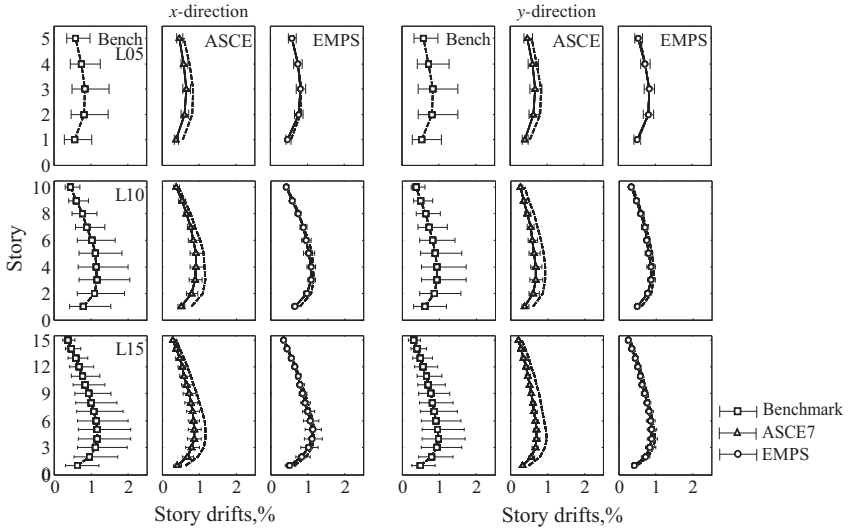

Fig. 10. Story drifts in percentage in x- and y-direction at corner c1 for L-plan structures. In each case the marker and the horizontal line represent the median value of the EDP ± σ, assuming a log-normal distribution.

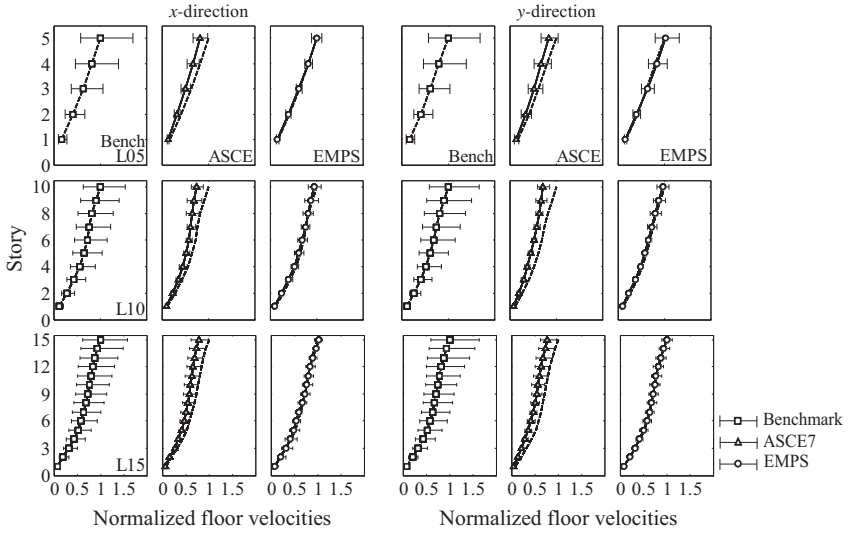

Fig. 11. Normalized floor velocities at the center of mass in x- and y-direction for L-plan structures. In each case the marker and the horizontal line represent the median value of the EDP ± σ, assuming a log-normal distribution.

similar results in y-direction. The markers and horizontal lines represent the median EDP value ± one standard deviation σ assuming a lognormal distribution.[1] For comparison purposes, the median benchmark values are kept in all sub-plots as a dashed line. In order to be consistent with comparisons of the EMPS procedure with the ASCE, geometric mean was used for the ASCE7 procedure although the ASCE7 requires mean. Use of "mean" instead of "geometric mean" do not affect the conclusions—provided that "mean" is consistently used for both scaling methods [39].

As demonstrated in Figs. 8 and 9, the records scaled according to the EMPS procedure provide median values of EDPs that are much closer to the benchmark values than is achieved by the ASCE7 scaling procedure; for example, compare columns 5 and 6 of Fig. 8. The maximum discrepancy of 30% in story drifts encountered by scaling records according to the ASCE procedure reduced to 10% when these records are scaled by the EMPS procedure; likewise, the maximum error in floor velocities is reduced from 26% for the ASCE7 scaling procedure to less than 7% for the EMPS procedure. The record-to-record variability is much less in EDPs due to a set of records scaled by the EMPS procedure (columns 3 and 6 of Figs. 8 and 9) compared to the records scaled by the ASCE7 procedure (columns 2 and 5 of Figs. 8 and 9). Small "record-to-record" variability increases the confidence level by indicating that records scaled appropriately with the target spectrum thus impose similar seismic demands. These results show that EDPs obtained from sets EMPS represent a considerable improvement in accuracy and efficiency variability when compared to EDPs obtained from sets ASCE7. Note that for these structures (without torsional irregularities $\beta < 1.2$), the ASCE7 procedure leads to large underestimations in story drifts and floor velocities.

6.2. L-plan structures

For L-Plan structures ($1.2 \leqslant \beta \leqslant 1.4$), the records scaled according to the EMPS procedure lead to more accurate estimates of

[1] 16th and 84th percentile values are computed as $\hat{\mu}e^{\pm\sigma}$, where $\hat{\mu}$ is the median value and σ is the standard deviation of a lognormal distribution.

median values of EDPs than ASCE7 scaling procedure. This improvement in accuracy is demonstrated in Figs. 10 and 11 where story drifts at corner c1 (Fig. 2) and normalized floor velocities at the center of mass due to records scaled and selected according to EMPS and ASCE7 procedures are shown together with benchmark values. For story drifts and floor velocities, ASCE7 procedure yields to over 20% errors in all cases. For this scaling procedure, the smallest error occurs when $\beta = 1.2$ (L10 building). The error in the EMPS procedure tends to decrease when the natural period of the structures increases. The maximum discrepancies encountered by scaling records according to the ASCE7 procedure are reduced when these records are scaled by the EMPS procedure; for example, the error in story drifts and floor velocities decreases from 28% to 8% and from 28% to 4%, respectively as compared to the benchmark values.

6.3. T-plan structures

Similar to the results for R- and L-plan structures, EDPs obtained from sets ASCE7 are less accurate than those obtained from EMPS. The ASCE7 procedure generally underestimates story drifts in lower stories and velocities in upper stories. In contrast, the EMPS procedure provides a more accurate estimate of story drift and floor velocity demands in all stories of these buildings because it considers structural strength and higher-"mode" contributions to the response; for example, compare columns 5 and 6 of Fig. 12. Even for T-plan structures with extreme torsional irregularities ($\beta > 1.4$), the EMPS procedure is highly accurate and efficient. For instance, compare columns 5 and 6 of Fig. 12 for building T10; for this building, the maximum discrepancy of 37% in story drifts encountered by scaling records according to the ASCE7 procedure is reduced to around 1% when these records are scaled by the EMPS procedure; the same behavior is evidenced by Fig. 13 where the discrepancy in floor velocities is reduced remarkably from 29% to 2%.

6.4. Other EDPs

Floor accelerations at the center of mass for the 5-story buildings are shown in Fig. 14. These accelerations are normalized by

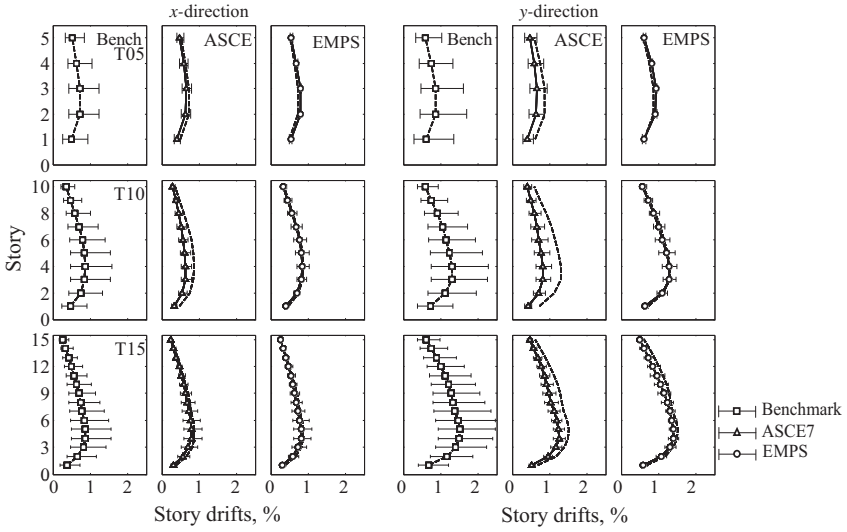

Fig. 12. Story drifts in percent in x- and y-direction at corner c1 for T-plan structures. In each case the marker and the horizontal line represent the median value of the EDP $\pm \sigma$, assuming a log-normal distribution.

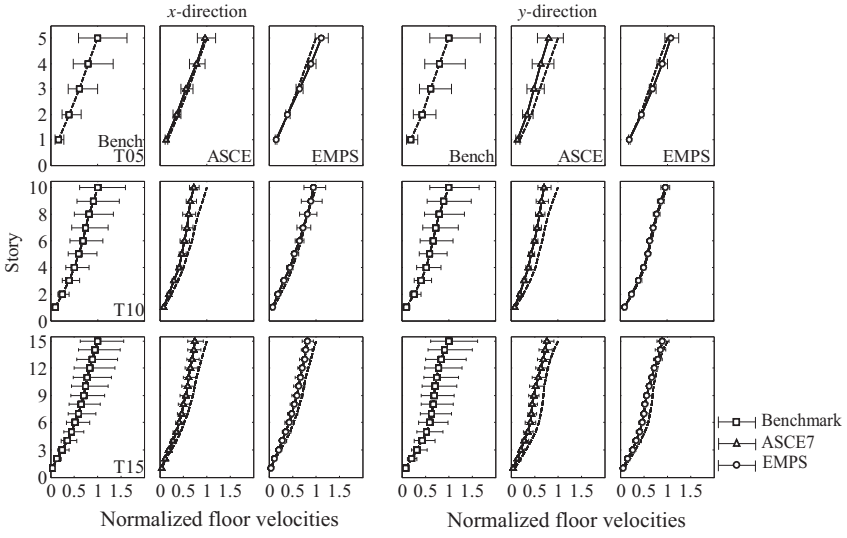

Fig. 13. Normalized floor velocities at the center of mass in x- and y-direction for T-plan structures. In each case the marker and the horizontal line represent the median value of the EDP $\pm \sigma$, assuming a log-normal distribution.

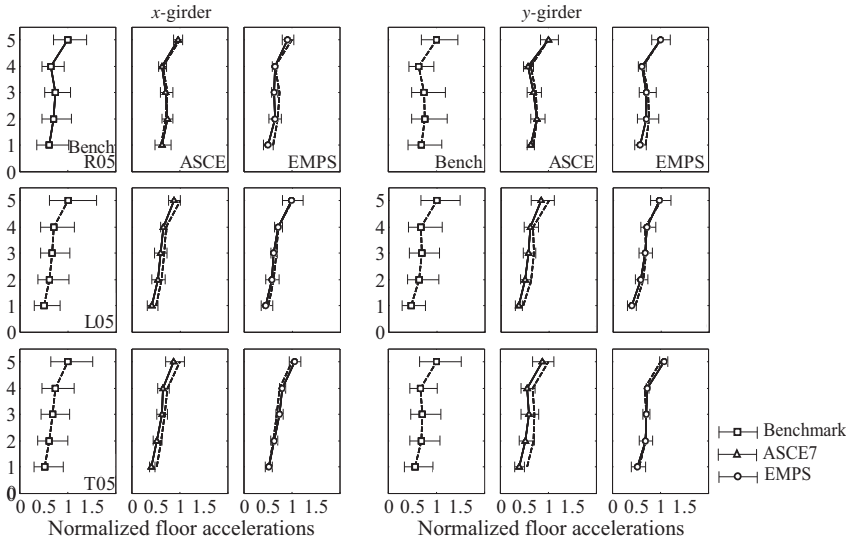

Fig. 14. Normalized floor accelerations in C.M. for 5-story buildings. For each set the marker and the horizontal line represent the median value of the EDP ± σ, assuming a log-normal distribution.

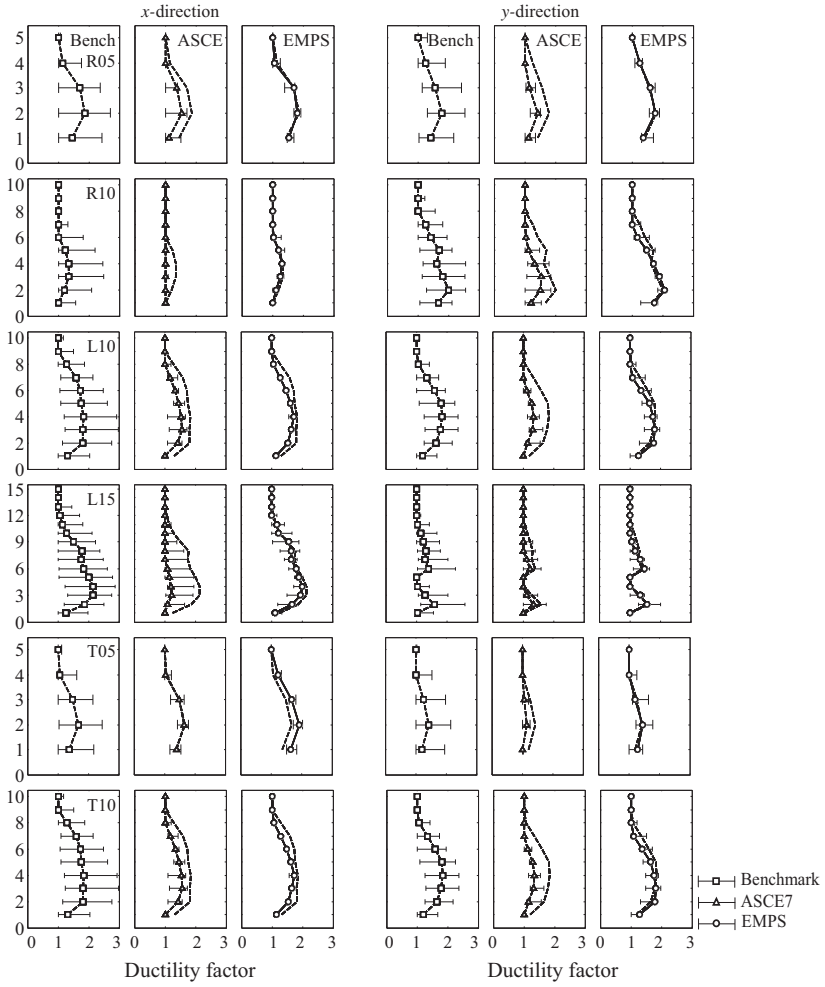

Fig. 15. Ductility factor in *x* and *y* girders for buildings R05, R10, L10, L15, T05 and T10 (figure). In each case, the marker represents the mean value of the EDP data and the horizontal line represents the interval of ductility demand values between the first and the third quartile of the data.

peak values occurred at any floor. Similar to the results shown previously, floor accelerations obtained from sets ASCE7 are less accurate than those obtained from EMPS. For R05 building the maximum discrepancy of 18% in floor accelerations encountered by scaling records according to the ASCE7 procedure is reduced to a maximum of 6% when these records are scaled by the EMPS

procedure. In the same way, for L05 and T05 buildings, the error is reduced from 15% to 2% and 20% to 9%, respectively. In this paper, representative results are shown; additional results are available in Refs. [40,41]. Note that even in regular structures (R-plan buildings) where the response is dominated by the first-"mode" of vibration (Fig. 3), the ASCE7 scaling procedure does not offer improvement in the demand estimates (columns 2 and 5 of Fig. 8).

Representative results for rotation ductility demands in girders for the following buildings: R05, R10, L10, L15, T05 and T10 are shown in Fig. 15 (due to space limitations, results for buildings R15, L05 and T15 are not shown); selected girders are highlighted in Fig. 2 by a diamond and triangle marker. Rotation ductility demands μ were calculated as $1+\theta_p/\theta_y$, where θ_p is the plastic hinge rotation and is θ_y the yield rotation. Because we found that μ is not log-normally distributed, the marker in Fig. 15 represents the median value of the EDP data and the horizontal line denotes the interval of ductility demand values between the first and the third quartile of the data. It is evident that maximum discrepancies encountered by scaling records according to the ASCE7 procedure are reduced when these records are scaled by the EMPS procedure. This figure confirms that the ASCE7 scaling procedure tends to underestimate ductility demands with errors between 20% and 43% in most cases. For building R05, the maximum discrepancy of 27% in ductility demands observed by scaling records according to the ASCE7 procedure, is reduced to around 1% when these records are scaled by the EMPS procedure; comparable results were obtained for building R10. For L-plan structures, the maximum error in buildings L10 and L15 decreases from 29% to 6% and from 43% to 8%, respectively. Similarly, for buildings T05 and T10, the maximum discrepancy of 21% and 28% in the ASCE procedure is reduced to less than 1% and 7%, respectively.

In summary, based on the results presented in Figs. 8–15, the extended EMPS procedure offers a sufficient degree of accuracy that should make it useful for practical application in estimating seismic demands—floor displacements, velocities, accelerations, story drifts, internal forces—for multi-story unsymmetric-plan buildings due to two horizontal components of ground motion applied simultaneously. By including structural strength and contributions of all significant modes of vibration, EMPS is able to adequately capture variation of EDPs.

7. Conclusions

In this study, the MPS procedure has been extended to multi-story unsymmetric-plan buildings in order to select and scale ground motion records to be used in nonlinear RHA. The accuracy of the extended MPS procedure was evaluated against the ASCE/SEI 7-10 scaling procedure by comparing the median values of engineering demands parameters (EDPs) due to a set of seven records scaled according to both procedures against the benchmark values. The efficiency of the scaling procedures was evaluated by computing the dispersions of the responses as a result of scaled ground motions; small dispersion indicates that the scaling procedure is efficient. A set of nine multi-story unsymmetric-plan buildings was selected for testing. This evaluation of the EMPS procedure has led to the following conclusions:

1. In the ASCE7 ground motion scaling procedure, the limit $1.5T_1$ is intended to consider period elongation due to stiffness degradation; however, even with this consideration, target spectral acceleration values used for scaling ground motions still remain elastic. EMPS procedure overcomes this issue by considering the inelastic target deformation value. The target value of inelastic deformation may be estimated by either (1) performing nonlinear RHA of the inelastic SDF system to obtain the peak deformation associated with each ground motion, and then computing the median of the resulting data set; or (2) multiplying the median peak deformation of the corresponding linear SDF system, known from the median response spectrum, by the inelastic deformation ratio, estimated from an empirical C_{Rn} equation (e.g., [19]). If there is lack of recorded motion for a specific hazard conditions, user may estimate the target deformation value using an empirical C_{Rn} equation.
2. Ground motion selection and scaling are two different processes. The ASCE7 scaling procedure does not consider spectral shape for ground motion selection; spectral shape is only considered for scaling to ensure that the average spectrum of scaled records is above the design spectrum between $0.2T_1$ and $1.5T_1$. However, in the EMPS procedure, spectral ordinates at higher-mode periods are considered effectively in selecting the final set of scaled records to be used in RHAs.
3. The extended MPS procedure is much superior compared to the ASCE7 procedure for scaling two components of ground motions. This superiority is evident in two respects. First, the ground motions scaled according to the EMPS procedure provide median values of EDPs that are much closer to the benchmark values than is achieved by the ASCE7 procedure. Second, the dispersion (or record-to-record variability) in the EDPs due to seven scaled records around the median is much smaller when records are scaled by the EMPS procedure compared to the ASCE7 scaling procedure. Small dispersion increases confidence.
4. In all cases, ASCE7 leads to underestimation of story drift, floor velocities and accelerations. Even for structures that respond dominantly in the first-"mode", the ASCE7 scaling procedure does not offer improvement in the demand estimate as compared to the benchmark results.
5. The ASCE7 procedure uses the same scaling factor for both components of ground motion; the use of the same scale factors for each component provides inaccurate estimates of the median EDPs in one or both horizontal directions. In contrast, the EMPS procedure allowing for different scaling factors for x and y components, provides an accurate estimate of the median EDPs and reduces the record-to-record variability of the responses.

References

[1] Lilhanand K, Tseng WS. Development and application of realistic earthquake time histories compatible with multiple-damping design spectra. In: Proceedings of the 9th world conference on earthquake engineering, vol. II, Tokyo-Kyoto, Japan; 1988. p. 819–24.
[2] Nau J, Hall W. Scaling methods for earthquake response spectra. J Struct Eng 1984;110:91–109.
[3] Kurama Y, Farrow K. Ground motion scaling methods for different site conditions and structure characteristics. Earthq Eng Struct D 2003;32(15):2425–50.
[4] Shome N, Cornell AC. Normalization and scaling accelerograms for nonlinear structural analysis. In: Proceedings of 6th U.S. national conference on earthquake engineering, vol. II, Seattle; 1998. p. 819–24.
[5] Shome N, Cornell CA, Bazzurro P, Carballo JE. Earthquakes, records, and nonlinear responses. Earthq Spectra 1998;14(3):469–500.
[6] Mehanny SSF. Modeling and assessment of seismic performance of composite frames with reinforced concrete columns and steel beams. PhD dissertation, Stanford University, CA; 1999.
[7] Alavi B, Krawinkler H. Consideration of near-fault ground motion effects in seismic design. In: Proceedings of the 12th world conference on earthquake engineering, paper no. 2665. Auckland, New Zealand; 2000.
[8] Bazzurro P. Probabilistic seismic demand analysis. PhD dissertation, Stanford University, CA; 1998.
[9] Shome N, Cornell CA. Probabilistic seismic demand analysis of nonlinear structures. Reliability of marine structures program. Report no. RMS-35; 1999.
[10] Baker JW, Cornell AC. Spectral shape, epsilon and record selection. Earthq Eng Struct D 2006;35(9):1077–95.
[11] Kennedy RP, Short SA, Merz KL, Tokarz FJ, Idriss IM, Power MS, et al. Engineering characterization of ground motion-task 1: effects of characteristics of free-field motion on structural response. Washington, DC: U.S. Regulatory Commission, NUREG/CR-3805; 1984.

[12] Malhotra PK. Strong-motion records for site-specific analysis. Earthq Spectra 2003;19(3):557–78.
[13] Alavi B, Krawinkler H. Behavior of moment-resisting frame structures subjected to near-fault ground motions. Earthq Eng Struct D 2004;33(6):687–706.
[14] Naeim F, Alimoradi A, Pezeshk S. Selection and scaling of ground motion time histories for structural design using genetic algorithms. Earthq Spectra 2004;20(2):413–26.
[15] Youngs R, Power M, Wang G, Makdisi F, Chin CC. Design Ground Motion Library (DGML) – tool for selecting time history records for specific engineering applications (abstract). SMIP07 seminar on utilization of strong-motion data; 2007. p. 109–110. <http://www.conservation.ca.gov/cgs/smip/docs/seminar/SMIP07/Pages/Paper8 _Youngs.aspx> [accessed 10/2009].
[16] Haselton CB, editor. Evaluation of ground motion selection and modification methods: predicting median interstory drift response of buildings. PEER ground motion selection and modification working group. PEER report 2009/01. Berkeley, CA: University of California; 2009.
[17] Bozorgnia Y, Mahin SA. Ductility and strength demands of near-fault ground motions of the Northridge earthquake. In: Proceedings of the 6th U.S. national conference on earthquake engineering, Seattle; 1998.
[18] Báez JI, Miranda E. Amplification factors to estimate inelastic displacement demands for the design of structures in the near field. In: Proceedings of the twelfth world conference on earthquake engineering, paper no. 1561. Auckland, New Zealand; 2000.
[19] Chopra AK, Chintanapakdee C. Inelastic deformation ratios for design and evaluation of structures: single-degree-of-freedom bilinear systems. J Struct Eng 2004;130(9):1309–19.
[20] Luco N, Cornell AC. Structure-specific scalar intensity measures for near-source and ordinary earthquake ground motions. Earthq Spectra 2007;23(2):357–92.
[21] Tothong P, Cornell AC. Structural performance assessment under near-source pulse-like ground motions using advanced ground motion intensity measures. Earthq Eng Struct D 2008;37(7):1013–37.
[22] Kalkan E, Chopra AK. Modal pushover-based ground motion scaling procedure for nonlinear response history analysis of structures. In: Proceedings of the Structural Engineers Association of California Convention, San Diego, California; 2009.
[23] Kalkan E, Chopra AK. Practical guidelines to select and scale earthquake records for nonlinear response history analysis of structures. U.S. Geological Survey Open-File Report 2010-1068. <http://pubs.usgs.gov/of/2010/1068/>.
[24] Kalkan E, Chopra AK. Evaluation of modal pushover-based scaling of one component of ground motion: tall buildings. Earthq Spectra 2012;28(4):1469–93.
[25] Kalkan E, Kwong NS. Documentation for assessment of modal pushover-based scaling procedure for nonlinear response history analysis of "Ordinary Standard" bridges. U.S. Geological Survey 2011. Open-File Report No: 2010-1328:56. <http://pubs.usgs.gov/of/2010/1328/>.
[26] Kalkan E, Kwong NS. Assessment of modal pushover-based scaling procedure for nonlinear response history analysis of "Ordinary Standard" bridges. ASCE J Bridge Eng 2012;17(2):272–88.
[27] Beyer K, Bommer JJ. Selection and scaling of real accelerograms for bi-directional loading: a review of current practice and code provisions. J Earthq Eng 2007;11(1):13–45.
[28] American Society of Civil Engineers (ASCE). Minimum design loads for buildings and other structures. ASCE/SEI 7-10, Reston, VA; 2010.
[29] Reyes JC, Chopra AK. Modal pushover-based scaling of two components of ground motion records for nonlinear RHA of buildings. Earthq Spectra 2012;28(3):1243–67.
[30] Reyes JC, Quintero O. Modal pushover-based scaling of earthquake records for nonlinear analysis of single-story unsymmetric-plan buildings. Earthq Eng Struct D 2013;43(7):1005–21.
[31] Chopra AK. Dynamics of structures: theory and applications to earthquake engineering. 4th ed. NJ: Prentice-Hall; 2007.
[32] Cornell CA, Jalayer F, Hamburger RO, Foutch DA. Probabilistic basis for 2000 SAC federal emergency management agency steel moment frame guidelines. ASCE J Struct Eng 2002;128(4):526–33.
[33] Chopra AK, Goel RK. A modal pushover analysis procedure to estimate seismic demands for unsymmetric-plan buildings. Earthq Eng Struct D 2004;33:903–27.
[34] Reyes JC, Chopra AK. Three-dimensional modal pushover analysis of buildings subjected to two components of ground motion, including its evaluation for tall buildings. Earthq Eng Struct D 2011;40:789–806.
[35] Reyes JC, Chopra AK. Evaluation of three-dimensional modal pushover analysis for unsymmetric-plan buildings subjected to two components of ground motion. Earthq Eng Struct D 2011;40:1475–94.
[36] Kalkan E, Kunnath SK. Effects of fling-step and forward directivity on the seismic response of buildings. Earthq Spectra 2006;22(2):367–90.
[37] Reyes JC, Kalkan E. Required number of ground motion records for ASCE/SEI 7 ground motion scaling procedure. U.S. Geological Survey Open-File Report No: 2011-1083. <http://pubs.usgs.gov/of/2011/1083/>.
[38] Reyes JC, Kalkan E. How many records should be used in an ASCE/SEI-7 ground motion scaling procedure. Earthq Spectra 2012;28(3):1205–22.
[39] Kalkan E, Chopra AK. Modal-pushover-based ground-motion scaling procedure. J Struct Eng 2011;137(3):298–310.
[40] Riaño AC. Selección y modificación de registros sísmicos para el análisis dinámico no lineal de edificaciones irregulares en planta de varios pisos – fase 1. Master thesis. Departamento de Ingeniería Civil y Ambiental, Universidad de los Andes, Bogotá, Colombia; 2013 [in Spanish].
[41] Arango CM. Selección y modificación de registros sísmicos para el análisis dinámico no lineal de edificaciones irregulares en planta de varios pisos – fase 2. Master thesis. Departamento de Ingeniería Civil y Ambiental, Universidad de los Andes, Bogotá, Colombia; 2013 [in Spanish].
[42] Reyes JC, Riaño AC, Kalkan E, Quintero OA, Arango CM. Assessment of spectrum matching procedure for nonlinear analysis of symmetric- and asymmetric-plan buildings. Eng Struct 2014;72:171–81.
[43] International Code Council (ICC). International Building Code. IBC 2009. West Flossmoor Road, Country Club Hills, IL; 2009.
[44] Computers and Structures (CSI), Inc. PERFORM 3D, user guide v4, non-linear analysis and performance assessment for 3D structures. Berkeley, CA: Computers and Structures, Inc.; 2006.
[45] ASCE/SEI. Seismic rehabilitation of existing buildings. ASCE/SEI 41-06, Reston, VA; 2007.
[46] Jayaram N, Baker J. Statistical tests of the joint distribution of spectral acceleration values. Bull Seismol Soc Am 2008;98(5):2231–43.